Sustainable Energy & Fuels

Supplementary information

Techno-economic assessment and Carbon footprint of processes for the large-scale production of Oxymethylene Dimethyl Ethers from Carbon Dioxide and Hydrogen

Received 00th January 20xx,
Accepted 00th January 20xx

DOI: 10.1039/x0xx00000x

Franz Mantei [a], Ramy E. Ali [a], Cornelie Baensch [b], Simon Voelker [c], Philipp Haltenort [d], Jakob Burger [e], Ralph-Uwe Dietrich [b], Niklas von der Assen [c], Achim Schaadt [a], Jörg Sauer [d] and Ouda Salem [a]*

1. Extended process description

1.1 Process routes P1 to P4 for the production of OME_{3-5}

The process chain of P1 to P4 starts from the production of MeOH which is synthesized from H_2 and CO_2 at 250 °C and 70 bar in the gas phase.[1] For the purification the reactor product enters a first flash unit at 65 °C and 65 bar, a second flash unit at 66 °C and 1 bar and a distillation column operated at 1 bar to separate MeOH and H_2O,[2] see Figure S1.

Process route P1

In the first process P1 one part of the MeOH is mixed with air and H_2O and used to synthesize FA in the gas phase via partial oxidation and dehydrogenation over a silver catalyst at 650 °C and 1 bar. Subsequently FA is separated using an absorber.[3] In the absorber column a wastewater stream is used to separate FA from the gas stream. Due to the high concentration of about 45 m/m% H_2O the product stream is concentrated to a FA rich stream containing about 86 m/m% FA and a H_2O rich stream containing about 10 m/m% FA which is partly used as washing liquid in the FA absorber.[4] The FA rich stream is mixed with the second part of the MeOH product and used as a feed stream for the production of OME_{3-5}. The synthesis of longer chain OME_n in the liquid phase at 80 °C and 2 bar in presence of an acidic heterogeneous catalyst like Amberlyst® 46 leads to a variety of side products which are separated in two distillation columns and a membrane unit to separate the side product H_2O.[5] The first distillation column operates at 1 bar and provides a bottom stream at 186 °C comprising mainly OME_{3-10} and a distillate stream at 64 °C which contains the rest of the components and a fraction of the total feed amount of OME_3 of about 42 %. The distillate stream is send to the membrane unit to separate H_2O from the mixture and recycled to the synthesis of OME_n.[6] The bottom stream is send to the second distillation column operating at 0.078 bar which provides the main product stream containing OME_{3-5} in the distillate at 80 °C and a bottom stream of OME_{6-10} at 196 °C which is recycled back to the OME_n synthesis. In comparison to the feed streams of MeOH and concentrated FA solution the mass flow of the recycled streams containing $OME_{1-3,6-10}$, MeOH, FA and a rest of not separated H_2O is about 5.4 times bigger. A simplified process flow sheet is shown in Figure S1.

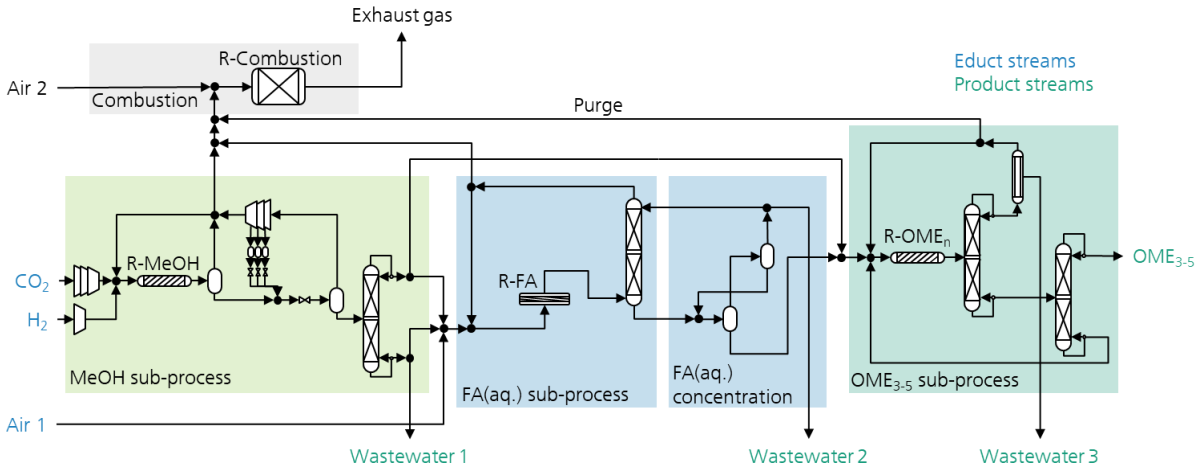

Figure S1 - Simplified process flow sheet for P1.

Process route P2

The second process P2 uses a part of the MeOH product saturated in a N_2 stream to certain desired concentration of 15 vol.-% to synthesize FA via dehydrogenation over Na_2CO_3 or $NaAlO_3$ at 900 °C and 2 bar and separate FA using an absorber and the second part of the MeOH product as washing liquid.[7,8] This separation of FA from the gas stream using an absorber with MeOH as washing liquid was adopted and adjusted from the FA(aqueous) sub-process which used H_2O instead. This concept was not yet described in the literature but due to the similar reaction system between MeOH and FA in comparison to FA and H_2O it is expected to yield a satisfying separation with probably slightly adjusted operational parameters. Furthermore, using H_2O as washing liquid is not a suitable strategy here since the advantage of an anhydrous FA stream would not be met.

The mixture contains about 63 m/m% FA and is used as a feed stream for the production of OME_{3-5}. This feed stream is converted to OME_{3-5} similar to the production of OME_{3-5} in P1. In comparison to P1, the amount of OME_3 lost in the first distillation column to the distillate product is about 27 %. Furthermore, the ratio of the mass flows of the recycled streams to the feed stream reduces to 4.4.

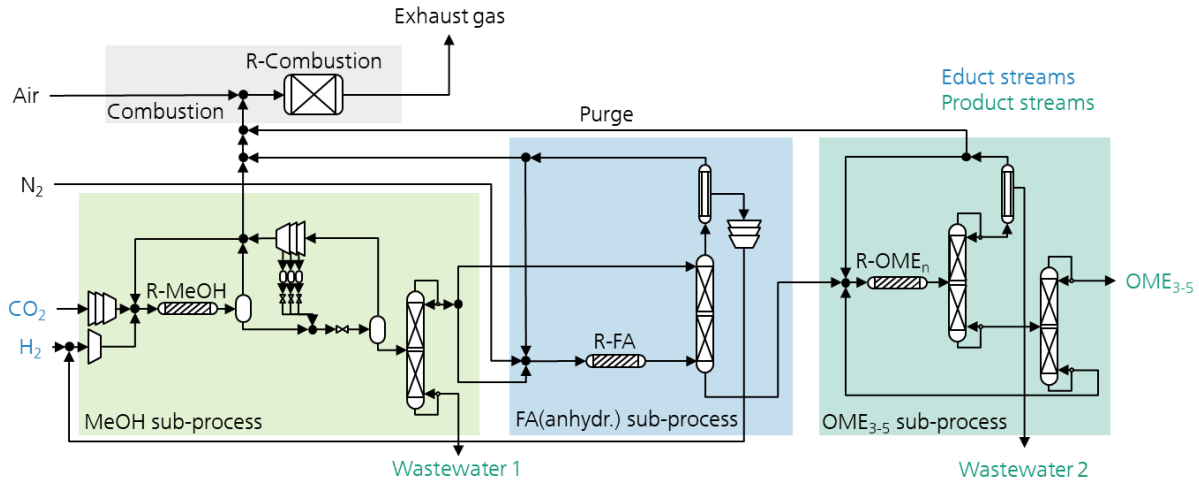

Figure S2 - Simplified process flow sheet for P2.

Process route P3

In the third process P3 a part of the MeOH product is used to produce FA following the FA(aqueous) sub-process. Parts of the product stream of the FA absorber is mixed with the second part of the MeOH product and used to produce OME_1. OME_1 is synthesized over an acidic heterogeneous catalyst like Amberlyst® 15 at 60 °C and 2 bar and purified using a series of a reactive distillation column with catalytic zones and a second distillation column.[3] The reactive distillation column is operated at 1 bar and produces a distillate stream containing an azeotropic mixture of OME_1 and MeOH with 94 m/m% OME_1 at 40 °C, a bottom stream containing mainly H_2O at 98 °C and a gaseous side stream below the catalytic zone containing 84 m/m% MeOH at 67 °C which is recycled back to the OME_1 reactor. The second distillation column splits the azeotropic mixture of OME_1 and MeOH at a higher pressure of 4 bar into a distillate stream containing the new azeotropic mixture of about 91 m/m% OME_1 and MeOH at 85 °C and an almost pure OME_1 bottom stream at 88 °C. The OME_1 product stream is mixed with the FA rich stream and used as a feed stream for the production of OME_{3-5}. The production of OME_{3-5} is similar to P1. In comparison to P1 the amount of OME_3 lost in the first distillation column to the distillate product is 37 %. Furthermore, in comparison to the feed streams the mass flow of the recycled streams is 4.8 times bigger.

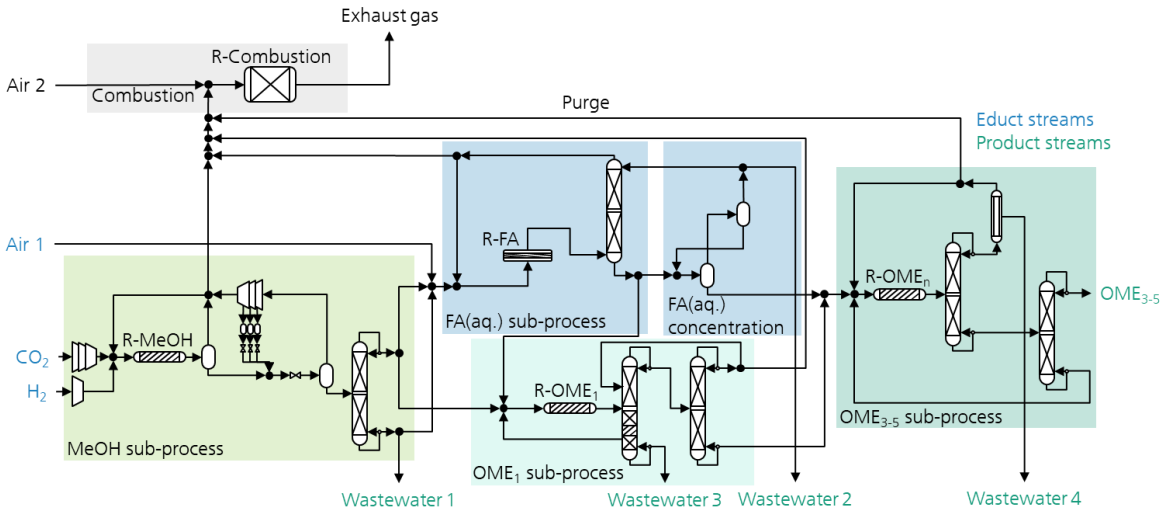

Figure S3 - Simplified process flow sheet for P3.

Process route P4

The fourth process P4 is a combination of P2 and P3 and uses one part of the MeOH product to produce FA following the FA(anhydrous) sub-process. One part of the product stream of the FA reactor is send to an absorber in which the second part of the MeOH product is used as a washing liquid and the product stream containing about 68 m/m% MeOH is send to the OME_1 sub-process. The absorption of the second part of the product stream of the FA reactor uses a recycled stream of the OME_{3-5} sub-process which mainly contains OME_{1-3}. This concept should be experimentally proven since the solubility of FA in OME mixtures not containing MeOH or H_2O was not yet investigated to the best of our knowledge. However, substituting the OME mixture with MeOH or H_2O is not a suitable strategy since their presence in the synthesis of longer chain OME_n would increase the side product formation, including H_2O. Therefore, the advantage regarding the H_2O separation unit in comparison to P1 to P3 would not be met. The product stream containing FA and a mixture of OME_{1-3} is mixed with the OME_1 product stream and used as a feed stream for the production of OME_{3-5}. The sub-processes of OME_1 and OME_{3-5} are similar to P3. The main difference is the amount of H_2O separated in the sub-process of the OME_{3-5} production. Starting from OME_1 and anhydrous FA only very small amounts of H_2O and MeOH enter this sub-process in form of impurities. However, to prevent accumulation H_2O needs to exit the process. Furthermore, only 31 % of OME_3 is lost in the first distillation column to the distillate product and the ratio between the mass flow of the feed stream and the recycled streams is reduced to 3.1.

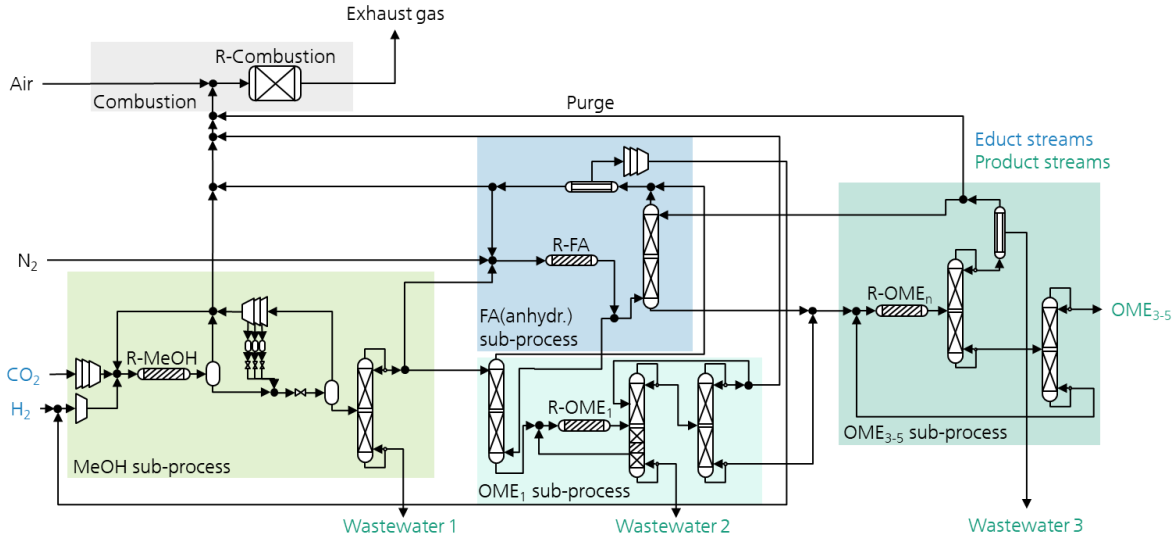

Figure S4 - Simplified process flow sheet for P4.

2 Process modelling and simulation

2.1 Pure component properties

Properties of the pure components used for the simulations are listed in Table S1.

Table S1 - Pure component properties.

Component	Parameter	Reference
CO, CO_2, FA, H_2, H_2O, MeOH, N_2, O_2, OME_1	c_p^{ig}, g_0, h_0, $\Delta_V h$, p_c, p^V, T_c, η, λ, ρ, σ	Aspen Database DB-PURE32
H_2, MeOH, OME_1, $OME_{3\text{-}5}$	LHV	[9]
HF_1	c_p^{ig}, g_0, h_0, p_c, T_c, η, λ, σ $\Delta_V h$, p^V	[3,10]
MG_1	c_p^{ig}, g_0, h_0, p_c, T_c, η, λ, σ $\Delta_V h$ p^V	[3,10–12]
HF_n, MG_n, n>1	c_p^{ig}, g_0, h_0, $\Delta_V h$, p_c, T_c, η, λ, σ p^V	[3,11]
OME_2-OME_{10}	c_p^{ig}, g_0, h_0, p_c, η, λ, σ $\Delta_V h$, p^V, T_c	[3,13]
OME_2-OME_5	ρ	[14]

2.2 Thermodynamic model for mixtures

A UNIFAC based model for mixtures containing FA, MeOH and H_2O was introduced by Maurer et al..[15] This model simultaneously considers the interactions between the components in the liquid phase and the chemical reactions between FA and MeOH as well as FA and H_2O yielding the formation of poly-(oxymethylene) hemiformals and poly-(oxymethylene) glycols according to OME_1 reactions (see eq. 9-13 in manuscript). Due to the fast kinetics of these reactions the assumption that the equilibrium composition will be reached instantaneously shows good agreement with the experimental results of vapor liquid equilibrium investigations. This model was further developed in the following decades adding new components like TRI and OME_n and adjusting the interaction parameters to new experimental data. Recently Schmitz et al.[16] published a new version of the model considering OME_n. Bongartz et al.[3] implemented the model version published by Kuhnert et al.[17] in Aspen Plus® and published the corresponding Aspen Plus® files. To include the chemical reactions of FA and MeOH as well as FA and H_2O Bongartz et al.[3] used the Chemistry section in Aspen Plus® which can be used to consider liquid phase equilibrium reactions. The UNIFAC interaction parameters were slightly reformulated to enable the implementation in Aspen Plus®, i.e. the temperature dependency was neglected, instead the values at 300 K were considered. In our work we used the Aspen Plus® model from Bongartz et al.[3] and adjusted it to consider the temperature dependency of the UNIFAC interaction parameters. Therefore, the model to calculate the liquid phase activity coefficient was adjusted to UNIFC-PSRK from the PSRK property model Gamma (GMUFPSRK) which enables the consideration of temperature dependent interaction parameters and showed slightly better results in the validation against experimental published results than the original model from Bongartz et al.[3], see Table S3. Furthermore, the UNIFAC parameters were adjusted to the ones published by Schmitz et al..[16] The equation of the temperature dependent UNIFAC interaction parameters for the sub-system H_2O and CH_2OH has the form of eq. 1, where $a_{i,j}$ is the UNIFAC interaction parameter of the sub-system i, here H_2O and j, here CH_2OH. A, B and C are the fitting parameters and T is the temperature in K.

$$a_{i,j}(T) = A + \frac{B}{T[K]} \tag{1}$$

$$a_{i,j}(T) = A + B \cdot T[K] + C \cdot T^2[K^2] \tag{2}$$

In Aspen Plus® the temperature dependency can be expressed according to eq. 2, therefore the equations where adjusted and refitted. The results are presented in Table S2 and Figure S5.

Table S2 - Refit of UNIFAC interaction parameters.

	A	B	C
$a_{2,8}$ Eq. (1), Literature	451.64	-114100	0
$a_{2,8}$ Eq. (2), Refit	-521.15	2.7288	-0.0025
$a_{8,2}$ Eq. (1), Literature	-1018.57	329900	0
$a_{8,2}$ Eq. (2), Refit	1794.1	-7.8899	0.0073

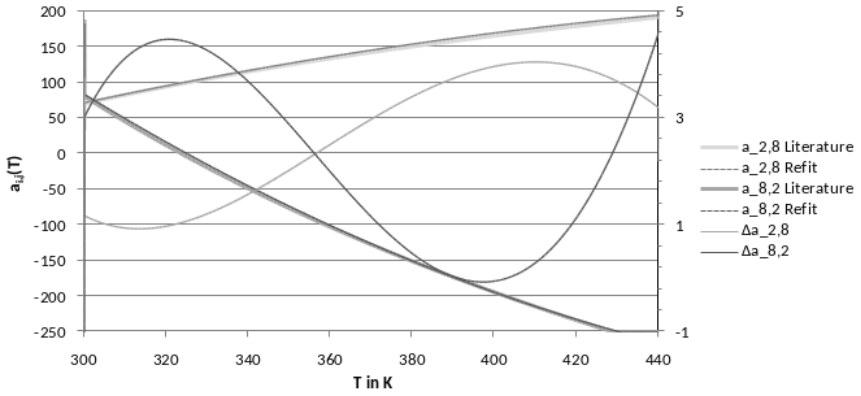

Figure S5 - Refit of UNIFAC interaction parameters.

Figure S5 shows a good agreement between the refitted equation of the UNIFAC interaction parameters and the equation from Schmitz et al..[16] Deviations are in a much smaller range than the values in the considered temperature range. The improvements regarding the description of the phase behavior is shown in Table S3.

2.3 Validation

For the validation of the implemented thermodynamic model describing the interactions in the liquid and vapor phase several experimental VLE data from different literature sources were used. The results are listed in Table S3.

Table S3 - Deviation of model predicted VLE data and experimental VLE data for four different models. The model Reference contains the model predictions from the literature sources presenting the experimental data. This work contains the model predictions from the model used for the process simulation in this work[3] contains the model predictions from the model published by Bongartz et. al.[3],[3]* contains the model predictions from the model published by Bongartz et. al.[3] and updated with the interaction parameters from Schmitz et. al.,[16] however still not considering the temperature dependency of the UNIFAC interaction parameters.

Sub-System	Reference	Data sets	Model	ΔAverage [%]	Δy_{FA} [%]	Δy_{MeOH} [%]	Δy_{H2O} [%]	Δy_{OME1} [%]	Δy_{OME2} [%]	ΔT [%]	Δp [%]
FA/ MeOH	18–20	54	Reference	3.0%	6.5%	1.0%	-	-	-	0.4%	4.1%
			This work	4.7%	10.9%	3.7%				0.3%	3.9%
			[3],[3]*	4.6%	10.7%	3.6%				0.3%	3.8%
				4.6%	10.7%	3.6%				0.3%	3.8%
FA/ MeOH/ H_2O	15,18,21–23	246	Reference	4.3%	6.9%	6.5%	6.1%	-	-	0.2%	2.0%
			This work	4.2%	7.4%	5.8%	5.5%			0.2%	2.2%
			[3],[3]*	5.6%	10.7%	7.8%	6.2%			0.3%	3.0%
				5.6%	10.7%	7.8%	6.2%			0.3%	3.0%
FA/ MeOH/ H_2O/ OME_1	10,24	45	Reference	21.1%	26.4%	19.7%	8.9%	67.7%	-	0.6%	3.4%
			This work	14.7%	26.1%	19.1%	10.9%	55.4%		0.8%	5.4%
			[3],[3]*	15.2%	27.9%	22.2%	8.8%	55.0%		0.6%	6.7%
				15.2%	27.9%	22.2%	8.8%	55.0%		0.6%	6.7%
FA/ MeOH/ H_2O/ OME_2	16	6	Reference	-	-	-	-	-	-	-	-
			This work	9.4%	27.6%	4.2%	15.8%		8.3%	0.2%	
			[3],[3]*	14.9%	38.0%	3.6%	23.8%		23.0%	0.6%	
				7.0%	26.0%	4.0%	3.5%		8.4%	0.2%	
FA/ MeOH/ OME_1	10	17	Reference	10.0%	16.3%	7.3%	-	10.2%	-	-	16.2%
			This work	11.6%	24.9%	4.7%		10.1%			18.1%
			[3],[3]*	11.1%	23.9%	4.4%		9.5%			17.5%
				11.1%	23.9%	4.4%		9.5%			17.5%

FA/ H_2O	10,15,18,25–29	312	Reference	2.3%	5.8%	-	1.1%	-	-	0.4%	1.9%
			This work	6.7%	7.6%		2.3%			14.9%	1.9%
			[3,3*]	6.5%	6.9%		2.3%			14.9%	2.1%
				6.5%	6.9%		2.3%			14.9%	2.1%
FA/ H_2O/ OME_1	10	26	Reference	21.8%	19.0%	-	13.9%	-	-	-	8.7%
			This work	19.6%	14.8%		15.2%				5.9%
			[3,3*]	20.2%	16.4%		14.9%				6.3%
				20.2%	16.4%		14.9%				6.3%
FA/ H_2O/ OME_2	16	6	Reference	-	-	-	-	-	-	-	-
			This work	10.3%	21.2%		22.6%		6.9%	0.6%	
			[3,3*]	9.6%	17.7%		23.0%		6.7%	0.6%	
				9.6%	17.7%		23.0%		6.7%	0.6%	
MeOH/ H_2O/ OME_1	30	23	Reference	5.0%	-	3.2%	13.4%	5.5%	-	0.2%	2.6%
			This work	5.3%		4.3%	12.7%	4.8%		0.3%	4.2%
			[3,3*]	5.2%		4.2%	13.4%	5.2%		0.3%	2.9%
				5.2%		4.2%	13.4%	5.2%		0.3%	2.9%
MeOH/ OME_1	10	63	Reference	1.4%	-	2.0%	-	2.1%	-	0.1%	1.4%
			This work	1.3%		2.0%		2.0%		0.1%	1.3%
			[3,3*]	1.8%		2.4%		2.3%		0.1%	2.4%
				1.8%		2.4%		2.3%		0.1%	2.4%
MeOH/ OME_2	31	22	Reference	-	-	-	-	-	-	-	-
			This work	1.6%		1.9%			4.6%	0.1%	
			[3,3*]	4.0%		4.2%			11.6%	0.4%	
				1.6%		1.9%			4.6%	0.1%	
H_2O/ OME_1	10	32	Reference	8.9%	-	-	14.0%	14.8%	-	0.2%	6.6%
			This work	7.1%			12.1%	12.9%		0.0%	3.5%
			[3,3*]	7.2%			12.8%	13.4%		0.1%	2.4%
				7.2%			12.8%	13.4%		0.1%	2.4%
OME_1/ OME_2	31	21	Reference	-	-	-	-	-	-	-	-
			This work	1.3%				1.4%	3.6%	0.2%	
			[3,3*]	0.8%				0.6%	2.4%	0.4%	
				0.8%				0.6%	2.4%	0.4%	

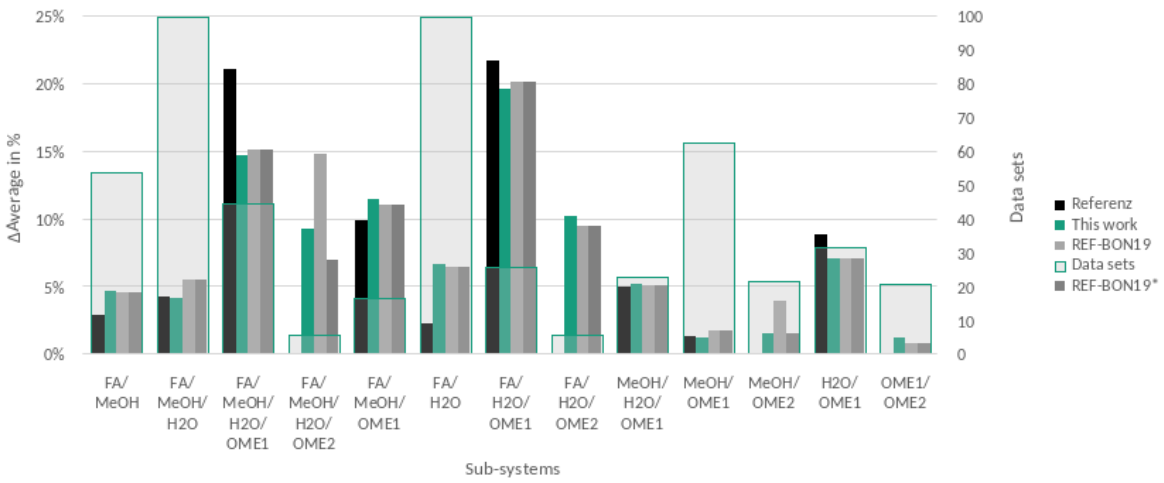

Figure S6 - Average deviation of VLE data from different sub-systems as presented in Table S3.

The validation was conducted using FLASH units in the simulation environment and running sensitivity studies with cases containing the experimental data from the respective literature sources. This procedure was chosen to enable the consideration of the formation of HF_n and MG_n in sub-systems containing FA, MeOH and H_2O. For the validation the overall composition was calculated considering HF_n and MG_n as individual FA, MeOH and H_2O molecules stoichiometrically. For a uniform procedure this approach was applied for sub-systems not containing FA as well.

Following this approach, the knowledge of the feed composition, pressure and temperature level is required. Since the experimental data usually only contain the composition of the liquid and the vapor phase as well as temperature and pressure level but no information regarding the mass distribution between liquid and vapor phase an assumption was made to define the feed composition. It was assumed that the feed composition is equal to the composition of the liquid phase. To keep the resulting error small the vapor fraction in the flash

unit was set to a small value of 1 x 10^{-4} to 1 x 10^{-5}, depending on the sub-system. The choice of the vapor fraction was based on the error between the resulting liquid phase composition to the liquid phase composition from the experimental data which was generally smaller 0.1 %, only in a few cases the error increases to 0.5%.

The results in Table S3 and Figure S6 show that the model predictions agree well with the experimental results. In addition to the deviations between the components, temperatures, and pressure themselves an average deviation is included enabling a fast comparison between different models. The deviations of the different models are generally very close to each other. A small improvement is visible for the model of This work and Bongartz et. al.,[3]* which is mainly a result of the updated model parameters from Schmitz et al..[16] The behavior of most of the sub-systems is described well by the model approach. However, systems containing the components FA/MeOH/H_2O/OME_1, FA/MeOH/H_2O/OME_2, FA/MeOH/OME_1, FA/H_2O/OME_1 and FA/H_2O/OME_2 show strong deviations of partly more than 20%. This is also the case for the Reference model which presents the model predictions published together with experimental data sets. Therefore, especially the predictions of the interactions between FA and OME show potential for improvement with improved experimental data sets.

2.4 Reaction systems

MeOH is synthesized from H_2 and CO_2 according to reactions (1)-(3) in the main script. The reactions were simulated in an isothermal plug-flow reactor considering the reaction kinetics by Nestler et. al.[1] and steam production for cooling.

FA(aqueous) is synthesized from MeOH and O_2 according to reactions (4)-(6) in the main script. The reactions were simulated in an adiabatic yield reactor assuming 98 % conversion of MeOH and a selectivity of 90 % towards FA.[3] FA(anhydrous) is synthesized from MeOH according to reactions (7) and (8) in the main script. The reactions were simulated in an isothermal yield reactor assuming 100 % conversion of MeOH and a selectivity of 70 % towards FA and 30 % towards CO.[7]

OME_1 is synthesized from MeOH and FA considering reactions (9)-(13) in the main script. The reactions were simulated in an isothermal plug-flow reactor. Reaction (9)-(12) proceed rapidly, therefore their equilibrium composition was simulated, independent of the length of the reactor. For reaction (13) the kinetic model by [32] was used by Bongartz et. al..[3] The formation of side products like dimethyl ether, trioxane and methyl format were not considered.

For the reactive distillation column only reaction (13) was considered on the trays containing catalyst, while reactions (9)-(12) were considered on the other trays. To facilitate the presentation of the results only the overall compositions are given in this work. Therefore, the compositions of HF_n and MG_n are considered as individual FA, MeOH and H_2O molecules. For more details see Schmitz et. al..[33]

OME_n is synthesized from MeOH, OME_1 and FA considering reactions (9)-(15) in the main script. The reactions were simulated in an isothermal plug-flow reactor. For reactions (13)-(15) the kinetic model from Schmitz et. al.[34] was used. The model was implemented using the Reaction class Custom in Aspen Plus® which cannot be used together with equilibrium models. Therefore, reaction (9)-(12) were implemented in kinetic models assuming a very fast conversion by adding a high factor to the model. Like the simulation of the OME_1 synthesis no side products were considered, and the results are presented in overall compositions.

2.5 Process component sizing

After the convergence of the heat integrated process simulations of P1-P4 the process unit operations were sized as a core step towards their cost evaluation. The applied approaches for the sizing of the different process unit operation types is described in the following.

Heat Exchangers

The area of the heat exchangers was sized using the heat flow $\dot{Q}$ calculated by Aspen Plus®, the logarithmic temperature difference ΔT_{ln} and the thermal transmittance U mainly for shell and tube heat exchanger suggested by[35] in following equation.

$$A_{\text{Heat Exchanger}} = \dot{Q}/(U \cdot \Delta T_{ln}) \quad (3)$$

This approach was used for all heat exchangers, condensers, and evaporators, including the ones from the distillation columns.

Reactors

The reactors were sized using the gas hourly space velocity GHSV, the weight hourly space velocity WHSV or a kinetic model.

The reactor for the methanol synthesis was sized using the kinetic model to estimate the volume of the reactive zone and assuming a pipe diameter of 38 mm, pipe length of 7 m and a void fraction of 0.4 according to Reza Zahedi et. al..[36] The number of pipes was adjusted to meet the reaction volume. To estimate the amount of catalyst required the density was estimated with 1775 kg/m^3.

For the reactions inside the FA synthesis reactor a GHSV of 15 000 h^{-1} was assumed.[37] This was assumed for both the aqueous and the anhydrous FA synthesis. The amount of catalyst required was estimated assuming a density of 1200 kg/m^3 and the volume of the reactor was estimated assuming a total volume of 3 times the volume required for the catalyst.

For the OME_1 and OME_n synthesis a WHSV of 30 h^{-1} was assumed.[34] With a catalyst density of 1100 kg/m^3 and a void fraction of 0.4 the reactor volume was defined. For the geometry of the pipes a diameter of 20 mm and a length of 10 m was assumed while the number of

pipes was adjusted to meet the required reaction volume. The dimensions of the applied Gibbs reactor for the combustion of the purge streams were defined by Aspen Process Economic Analyzer V11.

Distillation columns

Distillation columns were sized by Aspen Process Economic Analyzer V11 which estimates the dimensions of the column, a condensate accumulator, and a reflux drum pump. For the distillation columns in the MeOH, OME_1 and OME_n sub processes the columns were assumed to be packed with Beta rings (BX) packing. The absorber in the FA synthesis sub processes were assumed to be filled with Beta-rings and sieve trays.[38] Reboiler and condenser are heat exchangers and were estimated analogous to the other heat exchangers.

The absorption columns in the FA(anhydrous) step were assumed as ideal separation units in the simulation. For economic evaluation, their dimensions were estimated from the column dimension in the FA(aqueous) step assuming the same height and a diameter adapted to the corresponding mass flow according to $d_2 = d_1*(\dot{m}_2/\dot{m}_1)^{1/2}$.

Membrane

The membrane area of H_2 separation A_M was estimated based on the following assumptions:

- the membrane performance is independent of the membrane selectivity (pressure ratio limit),
- the pressure drop between feed inlet and retentate outlet is negligible,
- the residual H_2 mole fraction in the retentate is assumed 0.1, the H_2 mole fraction in the permeate is 0.9,
- The effective membrane area can be approximated by averaging the minimum and maximum area obtained from the feed (inlet) and retentate (outlet) conditions.

Thus, A_M was calculated according to:

$$A_M = \frac{y_{p,H2}\dot{n}_P}{\overline{P}_{M,H2}(x_{F/R,H2}p_R - y_{P,H2}p_P)}, \quad (5)$$

with the mole fraction of H_2 in the permeate $y_{p,H2}$ and in the feed $x_{F/R,H2}$, the mole flow of the permeate $\dot{n}_P$, and the pressure of the retentate p_R and the permeate p_P. The permeability of the membrane according to $\overline{P}_{M,H2}$ = 100 10^{-6}cm^3 (STP) cm^{-2} s^{-1} cm Hg^{-1} Baker et al.[39] was considered.

The membrane to separate H_2O in the OME_n sub-process was assumed to work similar to the PERVAP 4101 which was applied for H_2O separation of similar mixtures by Schmitz et. al.[6] published a simple equation to estimate the membrane area for the H_2O separation. This equation was used to size the membranes in the OME_n sub-processes of P1-P4. The membrane was simulated using an ideal separator which separates all the H_2O present in the feed mixture to the permeate. It was assumed that H_2O chemically bound in MG_n was not separated. Therefore, considering the overall concentrations the retentate still contains H_2O. The difference in H_2O concentration between the feed and the retentate was used to size the membrane area needed for the H_2O separation.

Multistage compressors

Multistage compressors are used in the MeOH sub-process. The sizing of the compression was conducted by Aspen Plus® and the sizing of the heat exchangers for intermediate cooling was implemented the same way the other heat exchangers were sized.

The other process unit operations were either dimensioned by Aspen Process Economic Analyzer V11, like pumps, compressors and flash units or neglected for the economic analysis, like valves, mixers, and splitters.

2.6 Process energy integration

The heat integration was conducted following the Pinch method using Aspen Energy Analyzer. Only heat exchangers were considered which do not transfer heat from or to heating or cooling utilities like e.g. the reactors for the MeOH and FA synthesis and the combustion and the heat exchangers for heating or quenching of the FA feed or product before or after the reactor. After the design of the heat exchanger network the flow sheet of the simulation was adjusted and step-by-step converged.

3 Process evaluation

3.1 Economic evaluation

Basic Assumptions and framework conditions

For a detailed listing of the general assumptions and conditions for the economic evaluation in this work see Table S4

Specific equipment cost

Specific equipment costs were preferably taken from Peters et al.,[40] if adequate. Another reference basis was chosen in the following cases:

- Multitube reactors
  According to the recommendation in Peters et al.[40] specific costs of floating head heat exchanger were taken for the specific cost of multitube reactors. In Peters et al.[40] a tube length and diameter dependent cost function for floating head heat exchangers is given. However, the tube lengths of up to 10 m in this work exceed the upper limit of 6 m in Peters et al.,[40] significantly, while no degression coefficient for a reasonable extrapolation is given. Hence, specific costs (only dependent on the surface area) were taken from Woods.[41] However, no pressure factor is given for floating head heat exchanger in this reference. To account for the reaction pressure of 70 bar in the MeOH synthesis step a pressure factor of 1.25 was assumed taken from a double pipe HEX in Woods.[41]
- Fixed-bed reactors
  Area surfaces of up to 22.8 m^2 were determined for the fixed bed reactors in the simulations. While the upper limit of 10 m^2 given in Peters et al.[40] would have resulted in a separation into 3 reactors, the upper limit of the surface area in Woods[41] of 500 m^2 is far above 22.8 m^2. This higher limit was assumed to be more reasonable for the current state of the art and specific fixed-bed reactor costs from Woods[41] were applied in this work.
- Thin film evaporators
  Sizing of the thin film evaporators revealed surface areas of up to 195 m^2. In the work of Deibele and Dohrn[42] an upper limit of 50 m^2 for the heat transfer area of thin film evaporators is given while the capacity in Peters et al.[40] only ranges up to 12 m^2 without stating a degression coefficient for the specific cost. Hence, specific costs and a degression factor were taken from Woods[41] assuming an upper capacity limit of 50 m^2.
- Membrane modules
  Membrane module costs are taken from Baker et al.[39] as no cost data for membranes are specified in Peters et al..[40] Ranges of manufacturing costs are given for different membrane module types in Baker et al..[39] High-pressure modules are generally more expensive than modules for low-pressure or vacuum application Baker et al..[39] As the latter are applied in this work the lower value of the price range is taken. Additionally, it is stated in Baker et al.,[39] that "the selling price is typically 2-5 times higher" than the manufacturing price. Hence, the manufacturing price was multiplied by the mean value of 3.5 for the calculation of the specific purchased equipment cost of membrane modules.

Specific cost of raw materials and utilities

Table S4 - Overview of specific cost of raw materials and utilities assumed in this work.

Raw material/utility	Specific cost	Unit	Reference
$Cu/ZnO/Al_2O_3$	95.24	€/kg	[43]
Silver	427.60	€/kg	Mean trading price in 2018[44]
Na_2CO_3	25	€/kg	Bulk estimation based on prices for small quantities from ref.[45]
Amberlyst 46	45	€/kg	Bulk estimation based on prices for small quantities from ref.[46]
N_2	12.5	€/t	[47]
Steam 4 bar			
Purchasing	22.8	€/t	[47]
Selling	16.0	€/t	[47] (70% of purchase price)
Steam 20 bar			
Purchasing	23.1	€/t	[47]
Selling	16.2	€/t	[47] (70% of purchase price)
Electricity	50	€/MWh	[47]
Compressed Air	0.02	€/m³	[48]
Cooling water	0.0035	€/m³	[49]
Wastewater	3.8	€/m³	[50]

Catalyst lifetimes

Table S5 - Overview of catalyst lifetimes assumed in this work.

Catalyst	Lifetime [months]	Ref.
$Cu/ZnO/Al_2O_3$	48	[51]
Silver	5.5	[37](range of 3-8 months given there, mean value taken)
Na_2CO_3	12	estimation
Amberlyst 46	12	estimation

Cost factors

Table S6 - Cost factors applied for the calculation of CAPEX.

CAPEX	Main equipment (Ref. [40])	Main compressors (estimated)	Basis
Direct cost factors			
Installation	0.47		EC
Instrumentation and control	0.36		EC
Piping system	0.68		EC
Electrical system	0.11		EC
Buildings	0.18		EC
Yard improvements	0.10		EC
Service facilities	0.70		EC
Indirect cost factors			
Engineering and supervision	0.33		EC
Construction expenses	0.41		EC
Legal expenses	0.04		EC
Contractor's fee	0.22		EC
Contingency	0.44		EC
Sum	**5.04**	**2.27**	
Working Capital	0.15	0.15	TCI
Interest rate	0.05	0.05	

Table S7 - Cost factors applied for the calculation of OPEX.

OPEX	Value	Basis	Ref.
Direct cost factors			
Operating supervision (OV)	0.15	OL	[52]
Maintenance labor (ML)	0.01	FCI	[40]
Maintenance material (MM)	0.01	FCI	[40]
Operating supplies (OS)	0.15	ML&MM	[52]
Laboratory charges	0.2	OL	[52]
Indirect cost factors			
Insurance and taxes	0.02	FCI	[52]
Plant overhead costs (PO)	0.5	TLC=OL+OV+ML	[40]
Administrative costs	0.25	PO	[52]

Results and discussion

Table S8 - Breakdown of the equipment costs calculated in this work.

	Purchased equipment costs [Mio€$_{2018}$]			
	P1	**P2**	**P3**	**P4**
Cost breakdown equipment type				
Compressors	7.7	13.3	7.6	9.4
Pumps	0.1	0.1	0.2	0.1
Heater/HEX	12.9	27.9	11.8	20.2
Reactors	4.3	4.4	4.6	4.6
Separators	4.0	3.7	4.3	6.2
SUM	**29.0**	**49.3**	**28.5**	**40.5**
Cost breakdown process steps				
MeOH sub-process	15.6	19.0	15.5	18.0
FA(aqueous/anhydrous) sub-process	7.7	25.9	6.3	16.2
OME_{3-5} sub-process	4.0	1.7	3.6	2.9
Heat recovery	1.6	2.6	1.7	1.9
OME_1 sub-process	--	--	1.3	1.5
SUM	**29.0**	**49.3**	**28.5**	**40.5**

Table S9 - Breakdown of the $OPEX_{R\&U}$ calculated in this work.

	Raw material/utility cost [Mio€$_{2018}$/a]			
	P1	**P2**	**P3**	**P4**
CO_2	60.33	67.26	59.78	67.98
H_2	113.32	88.55	112.30	89.57
N_2	--	0.25	--	0.25
$Cu/ZnO/Al_2O_3$	1.47	1.47	1.48	1.48
Silver (FA(aqueous)) / Na_2CO_3 (FA(anhydrous))	4.58	0.18	4.45	0.21
Amberlyst® 46	0.09	0.11	0.15	0.11
Wastewater	0.52	0.38	0.51	0.38
Steam, 20 bar	7.21	6.10	4.73	-1.16
Steam, 4 bar	-1.40	-1.02	1.82	4.84
Electricity	2.34	8.71	2.31	8.84
Compressed Air	5.14	5.41	5.17	5.72
Cooling water	0.20	0.14	0.14	0.12
SUM	**193.79**	**177.53**	**192.84**	**178.34**

Table S10 - Assumptions for economic evaluation in this work and in;[53] The lines highlighted in orange represent the adapted values for the comparison of the economic evaluations.

	This work	Reference	Schemme et al. [53]
Base year	2018	[47]	2017
Annual full load hours [h/a]	8000	[47]	8000
Plant operation time [a]	20	[47]	20
Plant capacity [MW]	66.25		300
Interest rate	5%	[47]	8%
LHV_{diesel} [MJ/l]	35.9	[54]	35.9
$LHVOME_{3-5}$ [MJ/kg]	18.9	[9]	19.22
CO_2 price [€/t]	309	[47]	70
H_2 price [€/kg]	4.2	[47]	4.6
CO_2 feed	25°C, 1 bar		25°C, 30 bar
H_2 feed	25°C, 30 bar		25°C, 30 bar
Cooling water			
Delta T [°C]	15-25	[47]	20-25
Cost [€/t]	0.0035	[49]	0.1
High pressure steam			
Conditions	220°C, 20 bar		250°C, 39.7 bar
Cost [€/t]	23.1	[47]	32
Medium pressure steam			
Conditions	150°C, 4 bar		175°C, 8.9 bar
Cost [€/t]	22.8	[47]	32
Low pressure steam			
Conditions	--		125°C, 2.3 bar
Cost [€/t]	--	[47]	32
Electricity cost [€/MWh]	50	[47]	97.6
η_{isen} compressors	80%		76%
η_{isen} pumps	80 % (70 % for reflux pumps)	[47]	60%
Max. compression ratio per stage	2.5-3		3
Min. temp. difference [K]	10		10
Pressure loss	100 mbar for reactors and separators, 340 mbar for HEX, 6.9 mbar per stage for columns > 1 bar, none for vacuum equipment	HEX: [55] columns: [56]	none

Table S11 - Comparison of ACC, OPEX and NPC from this work (with adapted assumptions according to Table S5 and from Schemme et. al..[53]

	This work (with adapted assumptions)			Schemme et al.[53]		
	ACC	$OPEX_{tot}$ [€$_{2017}$/l$_{DE}$]	NPC	ACC	$OPEX_{tot}$ [€$_{2017}$/l$_{DE}$]	NPC
P1/Route A	0.28	3.39	3.67	0.165	3.30	3.46
P2	0.48	2.99	3.47			
P3	0.27	3.42	3.69			
P4	0.40	2.99	3.39			
Route B (Trioxan + Methylal)				0.309	3.43	3.74
Route C (Trioxan + DME)				0.338	3.62	3.96

3.2 CO_2 footprint evaluation

Table S12 - LCA datasets for the comparison of the four OME_{3-5} routes.

Flow	Dataset	Region	Value	Reference
H_2	Polymer electrolyte membrane (PEM) electrolysis, 2018	DE	27.21 kg CO_2-eq./kg H_2	47
	Solid oxide electrolyzer cell (SOEC), 2018	DE	21.50 kg CO_2-eq./kg H_2	47
	Alkaline electrolysis (AEL), 2018	DE	26.09 kg CO_2-eq./kg H_2	47
	Hydrogen (steam reforming natural gas)	DE	See reference.	57
CO_2	Direct air capture (DAC), 2018	DE	-0.56 kg CO_2-eq./kg CO_2	47
	Monoethanolamine (MEA) cement, 2018	DE	-0.96 kg CO_2-eq./kg CO_2	47
Electricity	Power grid mix, 2018	DE	0.50 kg CO_2-eq./kWh$_{el}$	47
	Power grid mix, 2030	DE	0.31 kg CO_2-eq./kWh$_{el}$	47
	Power grid mix, 2050	DE	0.08 kg CO_2-eq./kWh$_{el}$	47
	electricity production, wind, 1-3MW turbine, onshore	DE	See reference.	58
Heat < 250°C	steam production, as energy carrier, in chemical industry	Europe	See reference.	58
Heat > 250°C	Electrode boiler	–	See reference.	59
	heat production, natural gas, at boiler modulating >100kW	Europe	See reference.	58
Cooling water	market for water, decarbonised	DE	See reference.	58
Wastewater	treatment of wastewater, average, capacity 1E9l/year	Europe	See reference.	58
Nitrogen	market for nitrogen, liquid	Europe	See reference.	58
Compressed air	market for compressed air, 600 kPa gauge	Europe	See reference.	58

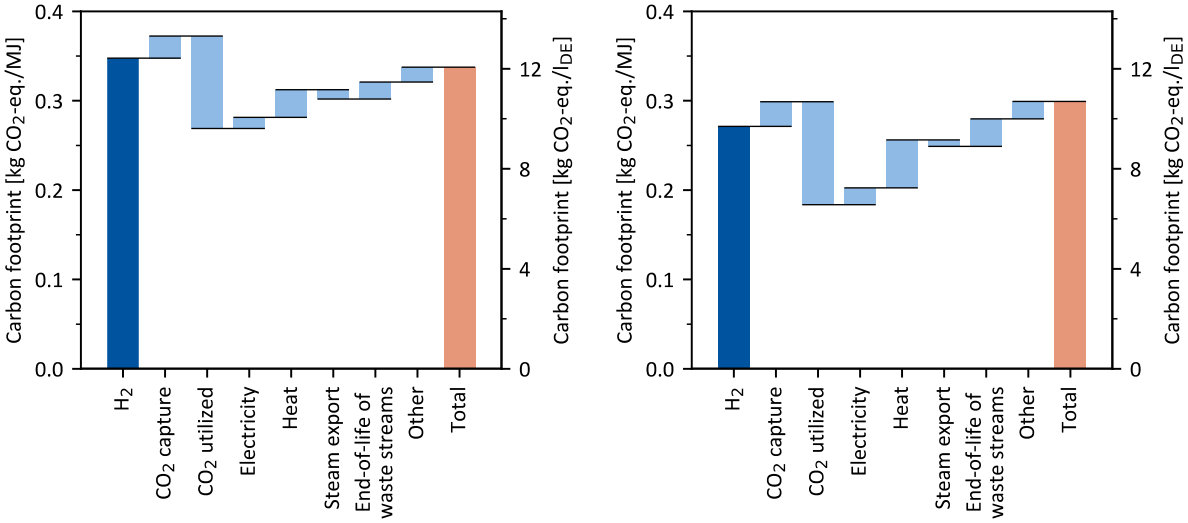

Figure S7 - Contribution analysis of the carbon footprint of the OME_{3-5} process routes P1 (left) and P2 (right) for the year 2018. The left y-axis shows the carbon footprint in kg CO_2-eq./MJ, while the right y-axis additionally indicates results in kg CO_2-eq./l_{DE}. The end-of-life of waste streams considers CO_2 in the exhaust gas and carbon carriers in the wastewater. Minor emissions due to wastewater treatment and the supply of cooling water, nitrogen, and compressed air are summarized as "other".

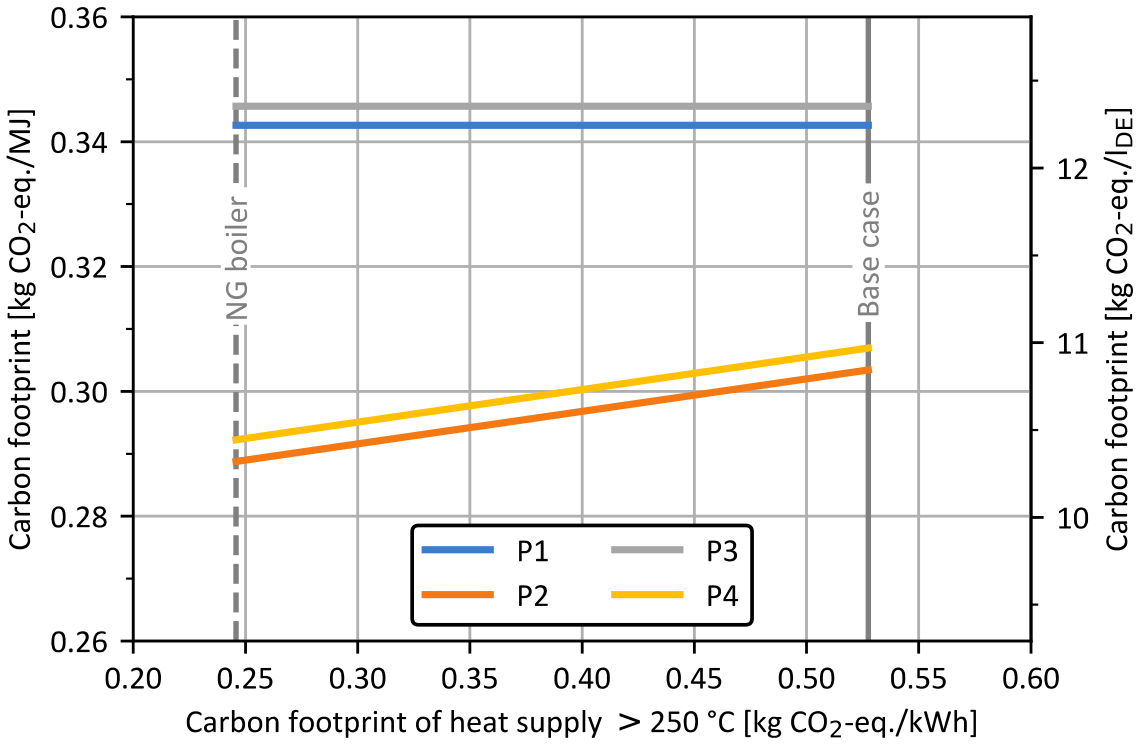

Figure S8 - Sensitivity analysis for the carbon footprint of all four OME_{3-5} process routes depending on the carbon footprint of high-temperature heat supply for the year 2018. The left y-axis shows the carbon footprint in kg CO_2-eq./MJ, while the right y-axis additionally indicates results in kg CO_2-eq./l_{DE}. NG boiler: natural gas boiler.[58]

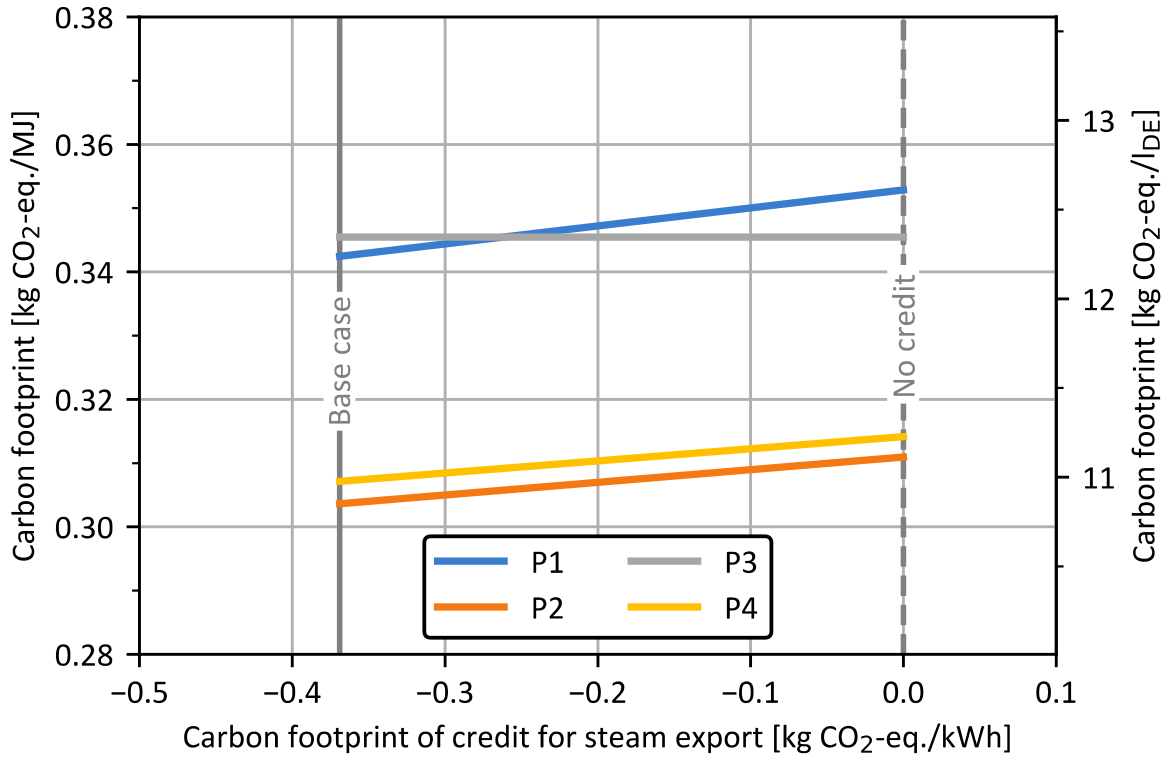

Figure S9 - Sensitivity analysis for the carbon footprint of all four OME_{3-5} process routes depending on the environmental credit, i.e., avoided burden, for steam export for the year 2018. The left y-axis shows the carbon footprint in kg CO_2-eq./MJ, while the right y-axis additionally indicates results in kg CO_2-eq./l_{DE}.

3.3 TRL evaluation

Table S13 - TRL levels used published in the energy research program of the German federal government.[60,61]

TRL	Definition
1	A basic principle has been scientifically observed, which can be considered for a technology/process/etc.
2	The functionality and possible applications of a technology/process/or the like has been scientifically described.
3	For individual elements of the technology/process (or similar), proof of function has been provided in a laboratory/test environment.
4	General function of the technology/process/etc. could be demonstrated in the laboratory/in a test environment
5	Technology/process/etc. has been implemented in an application-oriented overall system and general feasibility has been demonstrated
6	Demonstration plant/concept works in application-like environment
7	Prototype with system-relevant properties exists and is tested in the operating environment
8	Sales sample/prototype is available and meets all requirements of the end application
9	Commercial use

3.4 Evaluation Criteria Results

An overview of the process evaluation criteria namely process energy efficiency, NPC, CO_2 footprint and TRL of the four considered processes is summarized in the following web diagrams for the years 2018, 2030 and 2050

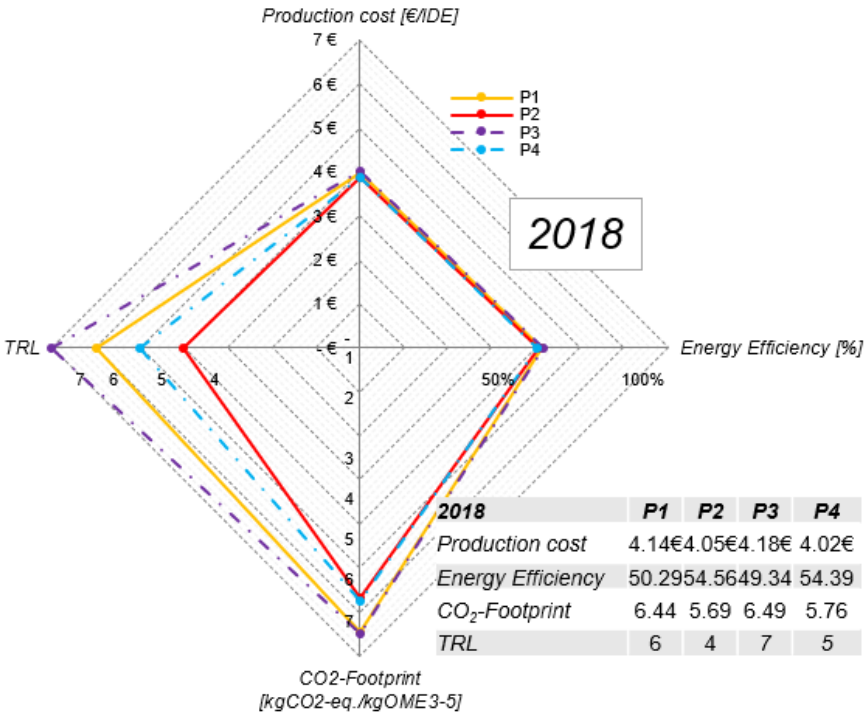

2018	P1	P2	P3	P4
Production cost	4.14€	4.05€	4.18€	4.02€
Energy Efficiency	50.29	54.56	49.34	54.39
CO_2-Footprint	6.44	5.69	6.49	5.76
TRL	6	4	7	5

Figure S10 - The base case scenario in 2018 main results represented in a web-diagram of all four $OME_{3\text{-}5}$ process routes; production cost in €/l_{DE}, energy efficiency in %, CO_2 footprint in kg CO_2-eq./$kg_{OME3\text{-}5}$ and TRL.

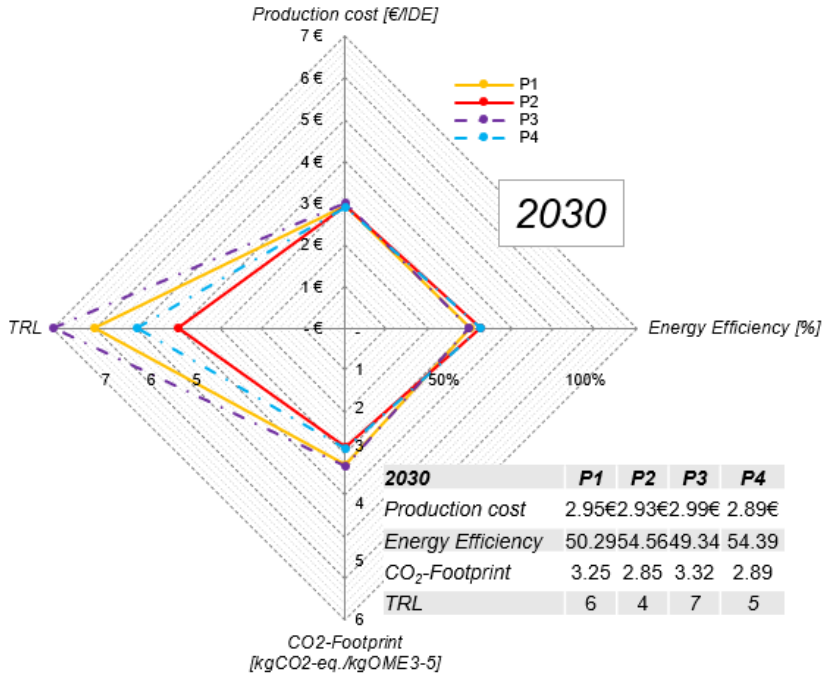

2030	P1	P2	P3	P4
Production cost	2.95€	2.93€	2.99€	2.89€
Energy Efficiency	50.29	54.56	49.34	54.39
CO_2-Footprint	3.25	2.85	3.32	2.89
TRL	6	4	7	5

Figure S11 - The base case scenario in 2030 main results represented in a web-diagram of all four $OME_{3\text{-}5}$ process routes; production cost in €/l_{DE}, energy efficiency in %, CO_2 footprint in kg CO_2-eq./$kg_{OME3\text{-}5}$ and TRL.

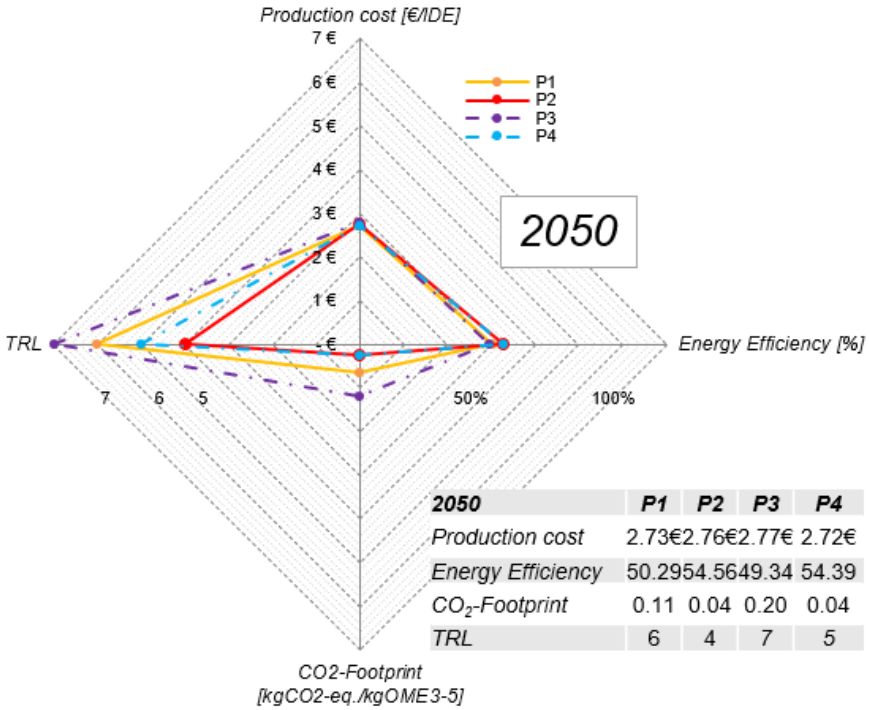

2050	P1	P2	P3	P4
Production cost	2.73€	2.76€	2.77€	2.72€
Energy Efficiency	50.29	54.56	49.34	54.39
CO_2-Footprint	0.11	0.04	0.20	0.04
TRL	6	4	7	5

Figure S12 - The base case scenario in 2050 main results represented in a web-diagram of all four $OME_{3\text{-}5}$ process routes; production cost in €/l_{DE}, energy efficiency in %, CO_2 footprint in kg CO_2-eq./$kg_{OME_{3\text{-}5}}$ and TRL.

Nomenclature

Abbreviations

Abbreviations	Full Name
ACC	Annual capital cost
CAPEX	Capital expenditures
CO	Carbon monoxide
CO_2	Carbon dioxide
DME	Dimethyl ether
EC	Equipment cost
FA	Formaldehyde
FCI	Fixed capital investment
H_2	Hydrogen
H_2O	Water
HF	poly(oxymethylene) hemiformals
KPIs	Key performance indicators
LHV	Lower heating value
MEA	Mono-ethanol amine
MeOH	Methanol
MG	poly(oxymethylene) glycols
N_2	Nitrogen
NPC	Net production costs
O_2	Oxygen
OME	Oxymethylene dimethyl ethers
OME_1	Methylal
OME_n	OME of chain length n
OPEX	Operational expenditures
$OPEX_{dir/ind}$	Direct and indirect operational expenditures
$OPEX_{R\&U}$	Raw material and utility costs

TCI	Total capital investment
TEA	Techno-economic assessments

Symbols and Indices

Symbol or Indices	Name
c_p^{ig}	Heat capacity of ideal gas
g_0	Standard free energy of formation
$\Delta_V h$	Enthalpy of vaporization
h_0	Standard enthalpy of formation
p_c	Critical pressure
p^V	Vapor pressure
T_c	Critical temperature
H	Dynamic viscosity
Λ	Thermal conductivity
ρ	Density
Σ	Surface tension
η_{Mass}	Mass efficiency
η_c	Carbon efficiency
η_{Energy}	Process energy efficiency
n	Order of the reaction
P	Pressure
T	Temperature
h_{labor}	Employee-hours per year
%	Percentage
l_{DE}	Liter diesel equivalent

References

1. F. Nestler, A. R. Schütze, M. Ouda, M. J. Hadrich, A. Schaadt, S. Bajohr and T. Kolb, Chem. Eng. J., 2020, **394**, 124881.
2. D. Bongartz, L. Doré, K. Eichler, T. Grube, B. Heuser, L. E. Hombach, M. Robinius, S. Pischinger, D. Stolten, G. Walther and A. Mitsos, Applied Energy, 2018, **231**, 757.
3. D. Bongartz, J. Burre and A. Mitsos, Industrial & Engineering Chemistry Research, 2019.
4. E. Ströfer, H. Hasse, K. Schilling and M. Sohn, Highly Concentrated Formaldehyde solution, Production and Reaction thereof(US 7,193,115 B2), 2007.
5. N. Schmitz, E. Ströfer, J. Burger and H. Hasse, Industrial & Engineering Chemistry Research, 2017, **56**, 11519.
6. N. Schmitz, C. F. Breitkreuz, E. Ströfer, J. Burger and H. Hasse, Journal of Membrane Science, 2018, **564**, 806.
7. J. Sauer and G. Emig, Chem. Eng. Technol., 1995, **18**, 284.
8. S. Su, P. Zaza and A. Renken, Chem. Eng. Technol., 1994, **17**, 34.
9. M. Held, Y. Tönges, D. Pélerin, M. Härtl, G. Wachtmeister and J. Burger, Energy Environ. Sci., 2019, **12**, 1019.
10. M. Albert, Thermodynamische Eigenschaften formaldehydhaltiger Mischungen, Shaker Verlag, Aachen, 1999.
11. H. Hasse, Dampf-Flüssigkeits-Gleichgewichte, Enthalpien und Reaktionskinetik in formaldehydhaltigen Mischungen, Universität Kaiserslautern, Kaiserslautern, 1990.
12. C. Kuhnert, Dampf-Flüssigkeits-Gleichgewichte in mehrkomponentigen formaldhydhaltigen [formaldehydhaltigen] Systemen, Shaker, Aachen, 2004.
13. J. Burger, E. Ströfer and H. Hasse, Chemical Engineering Research and Design, 2013, **91**, 2648.
14. D. Oestreich, Prozessentwicklung zur Gewinnung von Oxymethylenethern (OME) aus Methanol und Formaldehyd, Dissertation, KIT Scientific Publishing, 2017.
15. G. Maurer, AIChE J., 1986, **32**, 932.
16. N. Schmitz, C. F. Breitkreuz, E. Ströfer, J. Burger and H. Hasse, Chemical Engineering and Processing - Process Intensification, 2018. 10.1016/j.cep.2018.06.012.
17. C. Kuhnert, M. Albert, S. Breyer, I. Hahnenstein, H. Hasse and G. Maurer, Ind. Eng. Chem. Res., 2006, **45**, 5155.
18. H. Hasse and G. Maurer, Fluid Phase Equilibria, 1991, **64**, 185.
19. Y. M. Blazhin, L. K. Vagina, V. E. Pastor, A. I. Morozova and S. K. Ogorodnikov, In Zhur. Prikl. Khim. (49), pp. 174–178., 1976.

20. L. V. Kogan and S. K. Ogorodnikov, In JOURNAL OF APPLIED CHEMISTRY OF THE USSR 53 (1), pp. 98–102., 1980.
21. M. Albert, B. Coto García, C. Kuhnert, R. Peschla and G. Maurer, AIChE J., 2000, **46**, 1676.
22. S. J. Green and R. E. Vener, Ind. Eng. Chem., 1955, **47**, 103.
23. L. V. Kogan and S. K. Ogorodnikov, In JOURNAL OF APPLIED CHEMISTRY OF THE USSR 53 (1), pp. 102–105., 1980.
24. Z. Shan, Y. Wang, S. Qiu, C. Zheng and J. Shi, Fluid Phase Equilibria, 1995, **111**, 113.
25. C. Kuhnert, Dampf-Flüssigkeits-Gleichgewichte in mehrkomponentigen formaldehydhaltigen Systemen, Technischen Universität Kaiserslautern, 2005.
26. T. Grützner and H. Hasse, Journal of Chemical and Engineering Data - J CHEM ENG DATA, 2004, **49**. 10.1021/je030243h.
27. B. Olsson and Svensson, In Trans. Inst. Chem. Eng. (53), pp. 97–105., 1975.
28. Y. M. Blazhin, K. I. Valuev, L. V. Kogan, T. N. Tyvina and A. A. Kharchenko, In Zhur. Prikl. Khim. 50 (1), pp. 36–38., 1977.
29. L. V. Kogan, Y. M. Blazhin, S. K. Ogorodnikov and V. V. Kafarov, In Zhur. Prikl. Khim. 50 (12), pp. 2682–2687., 1977.
30. M. Albert, I. Hahnenstein, H. Hasse and G. Maurer, J. Chem. Eng. Data, 2001, **46**, 897.
31. Y. H. Song, J. Q. Li and J. F. Ding, Chem. Eng.(China), 2015, 30.
32. J.-O. Drunsel, M. Renner and H. Hasse, Chemical Engineering Research and Design, 2012, **90**, 696.
33. N. Schmitz, F. Homberg, J. Berje, J. Burger and H. Hasse, Industrial & Engineering Chemistry Research, 2015, **54**, 6409.
34. N. Schmitz, J. Burger and H. Hasse, Industrial & Engineering Chemistry Research, 2015, **54**, 12553.
35. VDI, VDI-Wärmeatlas: Mit 320 Tabellen, Springer Vieweg, Berlin, Heidelberg, 2013.
36. A. Elkamel, G. Reza Zahedi, C. Marton and A. Lohi, Energies, 2009, **2**, 180.
37. Ullmann's Encyclopedia of Industrial Chemistry, Wiley-VCH Verlag GmbH & Co. KGaA, Weinheim, Germany, 2012.
38. C. G. Braz, N. Lutters, J. Rocha, R. Alvim, E. Y. Kenig and H. A. Matos, Ind. Eng. Chem. Res., 2020, **59**, 5996.
39. R. W. Baker, Membrane technology and applications, J. Wiley, Chichester, New York, 2010.
40. M. S. Peters, K. D. Timmerhaus and R. E. West, Plant design and economics for chemical engineers, McGraw-Hill, Boston, 2003.
41. D. R. Woods, Rules of thumb in engineering practice, Wiley-VCH, Weinheim, 2007.
42. L. Deibele and R. Dohrn, eds., Miniplant-Technik in der Prozessindustrie, Wiley-VCH, Weinheim, 2006.
43. M. Pérez-Fortes and E. Tzimas, Techno-economic and environmental evaluation of CCU for fuel production: Synthesis of methanol and formic acid, 2016.
44. Silver price development in euro and dollar. https://www.gold.de/kurse/silberpreis/entwicklung/, (last accessed August 2021).
45. Sodium carbonate, ACS primary standard, 99.95-100.05% (dried basis), 33377. 2020, Thermo Fisher GmbH: Karlsruhe. https://www.alfa.com/de/catalog/033377/, (last accessed August 2021).
46. SigmaAldrich: Amberlyst 15(wet) ion-exchange resin, CAS 39389-20-3 2020, Merck KGaA: Darmstadt. https://www.sigmaaldrich.com/DE/de, (last accessed August 2021).
47. J. Prause, M. Raab, R.-U. Dietrich (2020), private communication. Framework assumptions TEA, Begleitforschung Energiewende im Verkehr (BEniVer).
48. R. Dindorf, Procedia Engineering, 2012, **39**, 204.
49. WasEG, Gesetz über die Erhebung eines Entgelts für die Entnahme von Wasser aus Gewässern (Wasserentnahmeentgeltgesetz des Landes Nordrhein-Westfalen - WasEG) [aw on the levying of a charge for the abstraction of water from bodies of water (Water Abstraction Charge Act of the State of North Rhine-Westphalia - WasEG]. 2004.
50. Bitterfeld-Wolfen, C., Preisblatt gemäß § 10 der AGB-E der Chemiepark BitterfeldWolfen GmbH [Price sheet according to § 10 of the AGB-E of Chemiepark BitterfeldWolfen GmbH], 2020. https://www.chemiepark.de/fileadmin/chemiepark_de/content/dokumente/preisblatt_agb-e_ab_2020.pdf, (last accessed August 2021).
51. Bartholomew, C.H. and Farrauto, R.J., Can. J. Chem. Eng., 2007, **85**, 127.
52. F. G. Albrecht, D. H. König, N. Baucks and R.-U. Dietrich, Fuel, 2017, **194**, 511.
53. S. Schemme, J. L. Breuer, M. Köller, S. Meschede, F. Walman, R. C. Samsun, R. Peters and D. Stolten, International Journal of Hydrogen Energy, 2020, **45**, 5395.
54. E. S. Heidrich, S. R. Edwards, J. Dolfing, S. E. Cotterill and T. P. Curtis, Bioresource technology, 2014, **173**, 87.
55. K. S. N. Raju, Fluid mechanics, heat transfer, and mass transfer: Chemical engineering practice, Wiley, Hoboken, N.J, 2010.
56. E. J. Henley and J. Seader, Equilibrium-stage separation operations in chemical, John Wiley and Sons Ltd, 1981.
57. V. Bouillon-Delporte, J. C., N. Brahy, Clean Hydrogen - Monitor 2020, Hydrogen Europe Intelligence Departement., 2020.
58. G. Wernet, C. Bauer, B. Steubing, J. Reinhard, E. Moreno-Ruiz and B. Weidema, Int J Life Cycle Assess, 2016, **21**, 1218.
59. L. J. Müller, A. Kätelhön, S. Bringezu, S. McCoy, S. Suh, R. Edwards, V. Sick, S. Kaiser, R. Cuéllar-Franca, A. El Khamlichi, J. H. Lee, N. v. d. Assen and A. Bardow, Energy Environ. Sci., 2020, **13**, 2979.
60. M. Héder, The Innovation Journal, 2018, **22**.

61. 7th Energy Research Programme of the Federal Government - Research for an environmentally-friendly, reliable and affordable energy supply. https://www.bmwi.de/Redaktion/EN/Artikel/Energy/research-for-an-ecological-reliable-and-affordable-power-supply.html, (last accessed June 2021).

